Environmental Science & Technology

Article

pubs.acs.org/est

Time Scales for Gas-Particle Partitioning Equilibration of Secondary Organic Aerosol Formed from Alpha-Pinene Ozonolysis

Rawad Saleh, Neil M. Donahue, and Allen L. Robinson*

Center for Atmospheric Particle Studies, Carnegie Mellon University, 5000 Forbes Avenue, Pittsburgh, Pennsylvania 15213, United States

Supporting Information

ABSTRACT: Most chemical transport models assume instantaneous equilibrium to represent gas-particle partitioning of semivolatile organic aerosol. This approach has been challenged by recent studies suggesting that secondary organic aerosol (SOA) cannot reach equilibrium within atmospheric time scales. The emergent hypothesis is that gas-particle partitioning rates are limited by diffusion within the condensed phase, which is thought to be "glassy." Here, we investigate the equilibration time scales of SOA formed from α-pinene ozonolysis by measuring the dynamic response to a modest step-change in temperature. Upon heating, equilibrium is disturbed, and the particles evaporate to restore equilibrium at the new temperature, which is attained when evaporation ceases. The SOA was formed at 10 °C and then heated to near room temperature (30 °C) so that the phase state (viscosity) of the condensed-phase after heating is similar to how it would be in the atmosphere. Experiments were performed in both a thermodenuder, with SOA loading of 350 μg/m^3, and in a smog chamber, with SOA loading of 2−12 μg/m^3. Both experiments show, contrary to previous findings, that the SOA achieves equilibrium with dynamic responses consistent with a mass accommodation coefficient of order 0.1. For typical atmospheric conditions, this translates into equilibration time scales on the order of minutes to tens of minutes, supporting the use of equilibrium partitioning in chemical transport models.

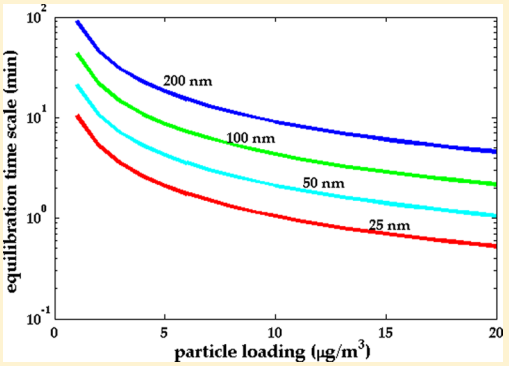

1. INTRODUCTION

It has been long established that a major portion of organic aerosol (OA) is comprised of semivolatile organic compounds (SVOCs), which partition between the condensed phase and the gas phase.[1−4] The extent to which they partition between the two phases, at equilibrium, is a function of their thermodynamic properties and is described by equilibrium partitioning theory.[5,6] The time scales over which an aerosol achieves equilibrium partitioning are governed by the kinetic properties of the aerosol, where thermodynamics plays a minimal role.[7,8] Most chemical transport models assume that partitioning kinetics are much faster than other atmospheric processes, which justifies treating atmospheric aerosols as being always at thermodynamic equilibrium, and using equilibrium partitioning theory to describe the gas-particle partitioning of SVOCs. However, recent studies have demonstrated that secondary organic aerosol (SOA) can exist in a highly viscous, semisolid, or glassy state.[9−11] Diffusion of molecules in this glassy matrix is thought to be very slow, which increases equilibration time scales enough to prevent SOA from reaching phase equilibrium on atmospherically relevant time scales.[12,13] This would entail complete rethinking of how OA partitioning is treated in chemical transport models.

These studies provide elegant measurements of evaporation rates, but a potential drawback in their interpretation is that evaporation rate is not equivalent to equilibration rate. While evaporation rate is governed by volatility and kinetic properties, equilibration rate is governed by the condensation sink of the aerosol[7,8] (see section 2.1). If an aerosol exhibits sluggish evaporation due to kinetic limitations (e.g., slow condensed-phase diffusion), that translates into slow equilibration; however, if the slow evaporation is due to low volatility, this has no implications on equilibration rate.

To interpret their evaporation rate data, Vaden et al.[12] and Cappa and Wilson[13] assume that the volatility distributions derived from smog chamber yield experiments[14] are valid. In such experiments, volatility distributions are fit to reproduce SOA yields at different precursor concentrations. However, monomers in SOA can form low-volatility oligomers in the condensed phase;[15,16] consequently, the volatility of the aged SOA may be considerably lower than the fresh SOA formed in yield experiments. Evaporation rate data do not distinguish between kinetic limitations (e.g., slow diffusion in the condensed phase) and the formation of low volatility oligomers, as the two phenomena have overlapping effects on evaporation rate. In other words, particles may evaporate very slowly simply because they are comprised of extremely low volatility

Received: January 7, 2013
Revised: May 1, 2013
Accepted: May 6, 2013
Published: May 6, 2013

   dx.doi.org/10.1021/es400078d | Environ. Sci. Technol. 2013, 47, 5588−5594

compounds and not because of a mass transfer limitation in the condensed-phase. This possibility was acknowledged by Cappa and Wilson.[13]

Here, we use the approach of Saleh et al.[7,17] to determine equilibration time scales of SOA formed from α-pinene ozonlysis. Our approach decouples the effects of thermodynamics and partitioning kinetics by characterizing the dynamic response (equilibration profile) of the aerosol system to a perturbation (step change in temperature). Therefore, equilibration time scales are directly observed, not inferred. We focus on the α-pinene SOA system because it was the model system used in the recent studies which concluded that the condensed phase exhibited diffusion limitations.[12,13,18]

2. METHODS

2.1. Theory. When a parcel of semivolatile aerosol, initially at equilibrium, is perturbed, the second law of thermodynamics forces the system to restore equilibrium via gas-particle partitioning. This is shown graphically in Figure 1, where

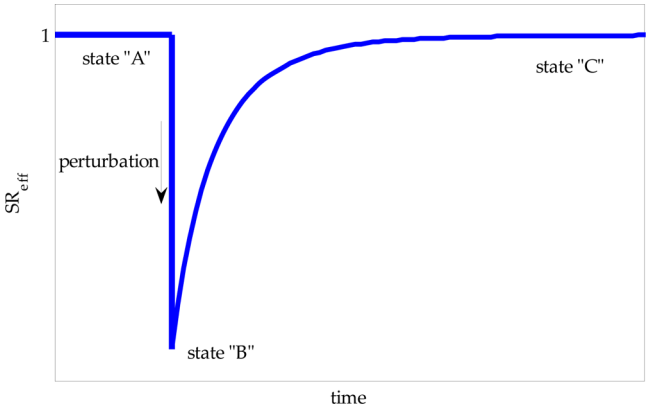

Figure 1. Illustration of a dynamic response (equilibration profile) of a semivolatile aerosol system to a perturbation (heating or dilution). The aerosol is initially at phase equilibrium (state "A"). It is perturbed to state "B" and then responds by partitioning toward the gas phase to bring itself back to equilibrium (state "C").

phase equilibrium is denoted by an effective saturation ratio (SR_{eff}) of unity. Here, we define SR_{eff} as the ratio of the total vapor concentration in the gas phase to the vapor concentration at equilibrium:

$$SR_{eff} = \frac{\sum C_{g,i}}{C_{sat,eff}} = \frac{\sum C_{g,i}}{\sum x_i \gamma_i C_{sat,i}} \quad (1)$$

where $C_{sat,eff}$ is the effective saturation concentration and x_i, γ_i, and $C_{sat,i}$ are the mole fraction, activity coefficient, and saturation concentration of component i.

The equilibration profile (the journey from the perturbed state (state "B" in Figure 1) to the new equilibrium state (state "C" in Figure 1) has the form of a dynamic response. Saleh et al.[17] showed that if the perturbation does not induce a large change in particle mass concentration (<20−30%), the dynamic response of a complex aerosol system is approximately first order:

$$SR_{eff} = 1 - e^{-t/\tau} \quad (2)$$

The e-folding time of the dynamic response (the equilibration time scale, τ) is given by[7]

$$\tau = \frac{1}{CS} = \frac{1}{2\pi D \sum_{i=1}^{n} F_i d_i N_i} \quad (3)$$

In this expression, CS is the condensation sink, D is the gas-phase diffusion coefficient, d is the particle diameter, N is the particle number concentration, n is the number of size bins, and $F = (1 + Kn)/(1 + 0.3773Kn + 1.33Kn(1 + Kn)/\alpha)$ is Fuchs−Sutugin correction factor for noncontinuum effects, where Kn is the Knudsen number and α is the mass accommodation coefficient.

Here, the definition of α is similar to that in Saleh et al.,[7,17,19] which is the ratio of molecular flux to/from the condensed-phase to the maximum theoretical flux predicted by kinetic theory. Thus, α subsumes all resistances to gas-particle partitioning (other than gas phase diffusion) including, but not limited to, (1) surface accommodation,[20] (2) deviation from Maxwell−Boltzmann molecular velocity distribution near the particle surface,[21] and (3) diffusion limitations in the condensed phase.[12,13] Consequently, if the condensed phase is highly viscous and exhibits substantial kinetic limitations, this would be manifested as a small α.

It is instructive to draw the analogy between the equilibration time scale and the time constant for charging a capacitor in the classic capacitor−resistor circuit, $\tau_C = RC$, where R is the resistance and C is the capacitance. The aerosol size distribution can be thought of as the capacitance of the aerosol system, and the kinetic properties as the mass transfer resistance to gas-particle partitioning. The aerosol size distribution can be easily measured, and D can, to first order, be estimated from the average composition of the condensing vapors.[22] However, the mass accommodation coefficient (α) cannot be derived from known molecular properties but has to be obtained experimentally. Once α of a certain aerosol type is determined, the equilibration time scales of this aerosol type at different conditions can be calculated using eq 3.

2.2. Experimental Section. *2.2.1. Approach.* Details of the experimental approach are described elsewhere,[7,17] and only a brief summary is given here. The perturbation scenario depicted in Figure 1 is reproduced experimentally to obtain equilibration profiles, by modestly heating the aerosol to initiate evaporation. It is essential that the system be closed such that upon evaporation, the vapor is allowed to build up in the gas phase to achieve equilibrium, as is the case in the atmosphere. In an open system (for example, if the vapor is continuously denuded from the gas phase), equilibrium will never be achieved (the particles keep evaporating until they disappear), and equilibration time scales cannot be measured. Saleh et al.[7,17] showed that the equilibration profile of a multicomponent aerosol can be traced in terms of an effective saturation ratio (SR_{eff}, defined in section 2.1). In the absence of gas-phase measurements of SVOCs, the equilibration profile can be determined experimentally from mass balance on the condensed phase (i.e., vapor build-up in the gas phase is calculated as the change in particle mass concentration):[7,17]

$$SR_{eff}(t) = \frac{\sum C_{g,i}(t)}{C_{sat,eff}(T_f)} = \frac{\Delta C_{OA}(t) + C_{sat,eff}(T_{in})}{\Delta C_{OA}(\text{equilibrium}) + C_{sat,eff}(T_{in})} \approx \frac{\Delta C_{OA}(t)}{\Delta C_{OA}(\text{equilibrium})} \quad (4)$$

dx.doi.org/10.1021/es400078d | Environ. Sci. Technol. 2013, 47, 5588−5594

where SR_{eff} is the effective saturation ratio defined in section 2.1, t is the time from perturbation, $C_{g,i}$ is the gas-phase mass concentration of component i, $C_{sat,eff}$ is the effective saturation concentration of the aerosol defined in section 2.1, T_f is the final temperature, T_{in} is the initial temperature, and ΔC_{OA} is the change in particle phase mass concentration.

The right-hand side of eq 4 assumes that $C_{sat,eff}(T_{in})$ is much smaller than $C_{sat,eff}(T_f)$, which is a good assumption if the temperature perturbation is large enough. In our experiments, T_{in} = 10 °C and T_f = 30 °C. For an enthalpy of vaporization of 100 kJ/mol, which is typical for atmospheric SOA,[3,23] $C_{sat,eff}(T_{in})/C_{sat,eff}(T_f)$ = 6%. Also, as shown in Saleh et al.,[17] using an equilibration profile of a complex aerosol system determines effective α to within 10% if the relative change in the particle mass concentration is less than 30%.

Two types of experiments were performed to quantify equilibration time scales of α-pinene SOA at mass loadings ranging over 2 orders of magnitude. The 2 orders of magnitude difference in loading creates a sizable difference in the composition of the condensed phase as more volatile compounds, which would be almost entirely in the gas phase at low loadings, partition significantly to the condensed phase at higher loadings.[5] We aim to investigate the effect of this difference in composition on equilibration time scales. The high loading experiments (~100 $\mu g/m^3$) are similar to previous studies which reported condensed phase diffusion limitations in α-pinene SOA,[12,13] while the low loading experiments (~1 $\mu g/m^3$) are more atmospherically relevant.

2.2.2. High Loading Experiments: Thermodenuder. SOA was generated from the ozonolysis of α-pinene (~ 40 ppb) with excess ozone (~ 800 ppb) in a 10 m^3 Teflon smog chamber. No seed aerosol was used. Throughout the experiment, the smog chamber was maintained at approximately 10 °C and less than 10% relative humidity. After the reaction was completed, SOA was drawn from the smog chamber into a thermodenuder (91.4 cm long, and 4.11 cm ID) with the wall temperature controlled to 30 °C. We chose to form the SOA below typical lab temperatures and to operate the thermodenuder at a low (but still atmospherically relevant) temperature specifically to examine the equilibration kinetics of the SOA at a phase-state similar to what would exist in the atmosphere. If the SOA is glassy under typical ambient conditions, it should be glassy in the thermodenuder. Initial and heated particle mass concentrations were determined by integrating the particle size distributions measured using a Scanning Mobility Particle Sizer (SMPS) and assuming a density of 1 g/cm^3. The equilibration profile was constructed by varying the aerosol flow rate to obtain different residence times in the thermodenuder.[7]

2.2.3. Low Loading Experiments: Chamber Heating. It is clearly desirable to measure equilibration under typical ambient conditions, not just temperature but also particle mass loading. One reason is that the semivolatile organics forming the SOA at higher loadings may be less prone to glass formation than the residue at lower loadings. However, low loading means a small condensation sink and thus a long equilibration time scale (eq 3). It is difficult to achieve equilibrium in a thermodenuder with low (atmospherically relevant) particle loadings[7,24,25] and is thus not possible to use a thermodenuder to obtain experimental equilibration profiles. To overcome this problem, we performed low loading temperature perturbation experiments in the smog chamber, where the aerosol can be allowed to equilibrate for several hours. SOA was generated in a similar fashion as described in the previous section, but with lower α-pinene concentrations (1 − 2.5 ppb). The smog chamber was initially controlled at 10 °C and less than 10% relative humidity. Approximately 1−2 h after initiating the ozonolysis, the smog chamber temperature was increased to 32 °C; throughout the experiment the particle size distributions were observed using an SMPS.

One challenge associated with performing equilibration experiments inside a smog chamber is the loss of particles by wall-deposition.[26] Since particle mass is lost due to both evaporation and deposition to the chamber walls, change in particle mass concentration (ΔC_{OA}) cannot be used as a metric for equilibration. In other words, due to wall-loss, even if the aerosol reaches equilibrium, C_{OA} does not level off. To overcome this problem, we characterize the dynamic response in terms of the evolution of the condensation sink diameter (d_{CS})[27] instead of C_{OA} (see SI for derivation of d_{CS}). Wall-loss and coagulation have a minor effect on the shape of the particle size distribution in these experiments; hence the change in d_{CS} can be assumed to be solely due to evaporation.

A second challenge with chamber equilibration experiments is that the chamber walls contribute to the effective condensation sink. While the condensation sink of the suspended aerosol can be readily calculated from the size distribution data, the condensation sink associated with the walls is much less certain. However, the influence of the walls can be bounded as discussed in section 3.2.

3. RESULTS AND DISCUSSION

3.1. High SOA Loading. Figure 2a presents equilibration profiles from four high SOA loading experiments. The initial C_{OA} in the smog chamber was 350 $\mu g/m^3$; however, the thermodenuder measurements were performed at lower C_{OA} due to wall-deposition. The C_{OA} in the four thermodenuder experiments was approximately 120, 80, 40, and 40 $\mu g/m^3$. When the C_{OA} dropped by wall-loss, the equilibrium partitioning was not disturbed and composition of the aerosol (both condensed-phase and gas-phase) did not change. Thus, the initial composition of the aerosol in each of the equilibration profiles in Figure 2a was the same. The count mean diameter (CMD) and the geometric standard deviation (σ_g) were approximately 130 nm and 1.35, respectively.

As evident in Figure 2a, the mass of evaporated SOA (ΔC_{OA}) increases with increasing residence time in the thermodenuder, and eventually levels off as the aerosol approaches equilibrium. ΔC_{OA} at each residence time can be normalized by $\Delta C_{OA,max}$ (or $\Delta C_{OA,equilibrium}$) to obtain an effective saturation ratio (SR_{eff}), where SR_{eff} = 1 denotes equilibrium (section 2.1). Since $\Delta C_{OA}/C_{OA,in}$ for all experiments is less than 20%, the dynamic response of the aerosol system to the step-change in temperature is approximately first order[17] and is defined by eq 2. The significance of this finding is that when plotted in nondimensional form (i.e., in SR_{eff} versus t/τ space), all data points in Figure 2a should fall on the (universal) first-order dynamic response curve, as shown in Figure 2b. This allows for a straightforward determination of the mass accommodation coefficient (α) since it is the only free parameter in the expression for τ (eq 2). Here, we obtained a value of α of 0.13. Note that in this fitting exercise, the position of the data points in t/τ space is adjusted (by optimizing the value of τ) to fit the dynamic response curve, and not the other way around. We reiterate that in nondimensional form, the dynamic response curve given by eq 2 is universal.

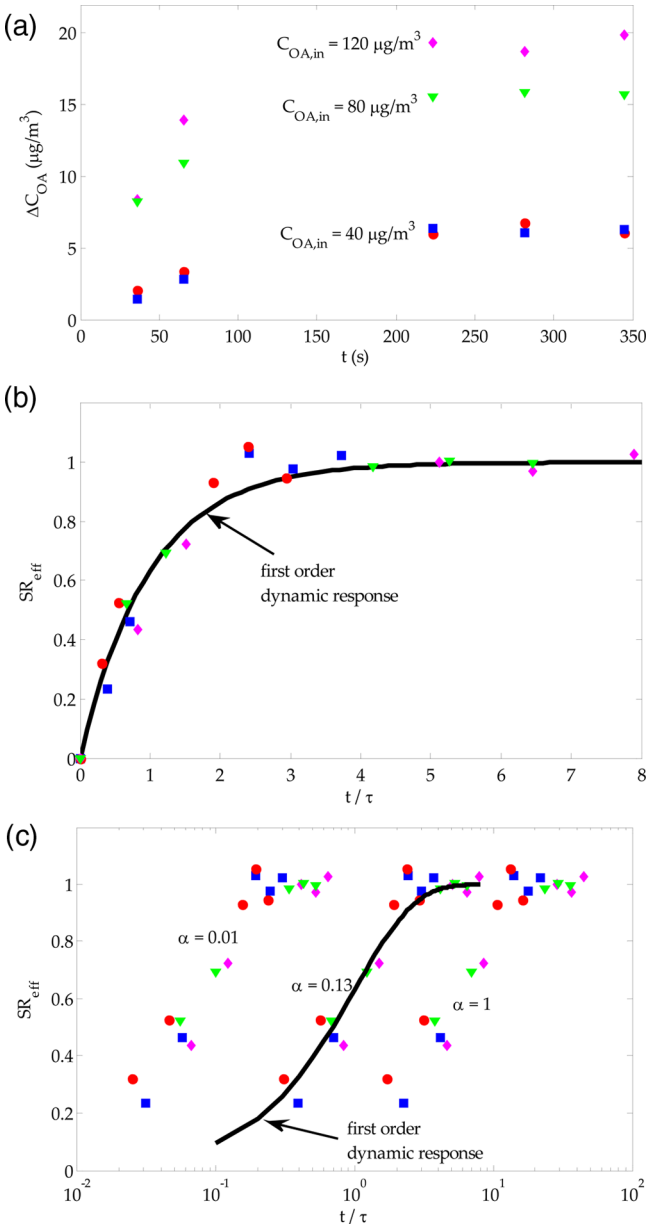

Figure 2. (a, top) Measured change in SOA particle mass concentration as a function of residence time in the thermodenuder. The aerosol was initially at 10 °C, and the thermodenuder was controlled to 30 °C. (b, middle) All data in Figure 2a plotted on nondimensional axes. The black curve is the first order dynamic response defined by eq 1. The position of the data points in t/τ space is adjusted to fit the (universal) dynamic response curve to determine an optimum value of α (0.13). (c, bottom) The same data points in Figure 2b plotted with τ calculated using different values of α. It is evident that fitting the measurements to the dynamic response provides a good constraint on α.

The value of τ, and thus the position of the data points in t/τ space (Figure 2b), is highly sensitive to the value of α. Consequently, fitting experimental equilibration profiles to the dynamic response curve provides a strong constraint on α. To illustrate, Figure 2c shows that when the data points are plotted with τ calculated using α of 0.01 and 1, they deviate significantly from the universal dynamic response curve. Clearly, α is well constrained.

The base case α values were calculated assuming an average molecular mass (M) and diffusion coefficient (D) of 200 g/mol and 5 × 10^{-6} m^2/s, respectively. A larger D reduces α, while a larger M increases α (see Supporting Information). To investigate the sensitivity of α to the values of M and D, we varied them by 50% each and estimated an upper bound (for M = 250 g/mol and D = 2.5 × 10^{-6} m^2/s) and a lower bound (for M = 100 g/mol and D = 7.5 × 10^{-6} m^2/s) of α. As shown in Table 1, the combined 50% change in M and D leads to an approximately 30% change in α. This range of M and D was chosen to encompass values for C_3 to C_{10} dicarboxylic acids. Note that as long as consistent α, D, and M values are used, the calculated equilibration time scales are the same.

Table 1. Mass Accommodation Coefficient Values Found in This Study for α-Pinene SOA for Different Assumptions on Gas Phase Diffusion Coefficient and Molar Mass

	mass accommodation coefficient (α)		
	D = 5 × 10^{-6} m^2/s, M = 200 g/mol (base case)	D = 7.5 × 10^{-6} m^2/s, M = 100 g/mol	D = 2.5 × 10^{-6} m^2/s, M = 250 g/mol
high loading (350 μg/m^3)	0.13	0.09	0.17
low loading (<12 μg/m^3)	0.15	0.1	0.2

3.2. Low SOA Loading. In this section, we present data from the chamber perturbation experiments performed at much lower (atmospherically relevant) particle loadings (2−12 μg/m^3). Because C_{OA} in the smog chamber decreases due to not only evaporation but also wall-loss, the dynamic response of the aerosol system was traced in terms of the evolution of the condensation sink diameter (d_{CS})[27] instead of C_{OA}. The d_{CS} and σ_g of the particle size distributions ranged between 45 and 60 nm and 1.25 and 1.4, respectively. Typical experimental data are shown in Figure 3. The aerosol was initially at equilibrium (at 10 °C), demonstrated by a constant d_{CS}. At time = 0 h, the temperature in the chamber was increased to 32 °C, and the particles responded by evaporating, which is evident from the decrease in d_{CS}. After ∼1 h, d_{CS} leveled off, indicating that the system achieved equilibrium. Since the temperature ramp (∼10

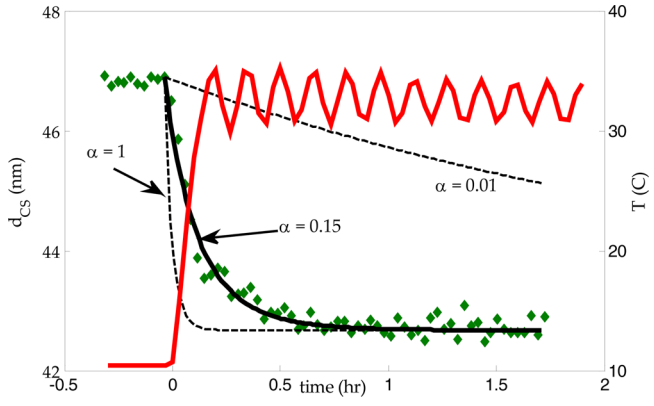

Figure 3. Data from a chamber perturbation experiment (heating at low SOA loading). Red trace is the temperature in the chamber (right y axis). Green diamonds represent the evolution of the condensation sink diameter determined from the SMPS data (left y axis). Black curves are partitioning kinetics model simulations with different α values. It is evident that the optimum α is well-constrained.

dx.doi.org/10.1021/es400078d | Environ. Sci. Technol. 2013, 47, 5588−5594

min) was much shorter than the dynamic response of the aerosol system (~1 h), the temperature ramp approximated a step function. The fact that the temperature ramp was not exactly a step function results in a slight overestimation of equilibration time scales (underestimation of α) but does not alter the conclusions of this work.

To determine the value of α, the measured evolution of d_{CS} is fit with a partitioning kinetics model.[7] This problem is complicated by the unknown contribution of wall-bound particles (particles which deposit on the chamber walls in the course of an experiment) to vapor build-up in the gas phase. There are two limiting cases: (1) the wall-bound particles do not contribute to vapor build-up, and (2) the contribution of wall-bound particles to vapor build-up is the same as suspended particles. Reality lies somewhere in between. To account for the contribution of the wall-bound particles, an additional condensation sink term ($w \times CS_{wall}$) is incorporated in the partitioning kinetics model. CS_{wall} is the condensation sink of the wall-bound particles (see Supporting Information for estimation of CS_{wall}), and w is a correction factor. $w = 0$ and $w = 1$ correspond to the first and second limiting cases described above. The smog chamber was thoroughly cleaned between experiments by flushing with clean air while heating to ~50 °C, and UV-lights are turned on for at least 24 h. Thus, we assume that CS_{wall} of residual particles from previous experiments is negligible.

We performed partitioning kinetics simulations with values of w between 0 and 1. Using $w = 0$ in the partitioning kinetics model yields an upper bound on α because the capacitance of the aerosol system is maximized (only suspended particles are a source of vapors), thus the resistance to gas-particle partitioning has to be minimized in the model to match observation. $w = 1$ yields a lower bound on α because the capacitance of the aerosol is minimized. The true value of α lies somewhere in between.

To constrain the true α (and w), we performed experiments with varying CS_{sus}-to-CS_{wall} ratios by allowing different amounts of wall-loss to occur before performing the temperature perturbation. The larger the ratio, the greater the difference between the upper and lower bounds on α, because the partitioning kinetics model results are more sensitive to w. If the modeled α is plotted versus w for different experiments (with varying CS_{sus}-to-CS_{wall} ratios), all the curves should intersect at the true α and w. This is shown in Figure 4. The model curves intersect at $0.2 < w < 0.3$, and an α of approximately 0.15, which is consistent with the high concentration thermodenuder data.

Figure 3 shows partitioning kinetics simulations with an α of 0.15 (the optimum value), 1, and 0.01. It is obvious that an α of 1 and 0.01 cannot reproduce the experimental data and that the optimization process yields a good constraint on α. Similar to the high loading experiments, the base case α values were obtained with the assumption that the average molecular mass (M) and diffusion coefficient (D) of the SOA were 200 g/mol and 5×10^{-5} m^2/s, respectively. We used the same procedure described in section 3.1 to estimate the sensitivity of α to M and D. The results are presented in Table 1.

Vapor loss to the chamber walls can influence interpretation of smog chamber experiments. There are three phenomena that can lead to vapor loss to the chamber walls: (1) if the walls are highly adsorptive, they would act as a sink for the vapors; (2) if the vapors in the chamber are supersaturated, the walls act as condensation sites; (3) vapors can be lost to the walls by absorptive partitioning (Matsunaga and Ziemann[29]). We address each of these issues in turn.

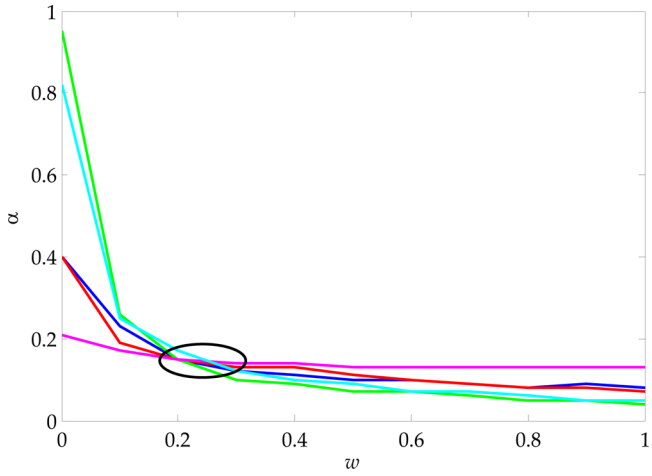

Figure 4. Calculated mass accommodation coefficients as a function of assumed contribution of wall-bound particles to vapor build-up in the gas phase (w). The curves correspond to experiments with different CS_{sus}-to-CS_{wall} ratios (see section 3.2). The magenta and the green curves have the lowest and highest CS_{sus}-to-CS_{wall} ratios, respectively. All curves intersect at an optimum α of 0.15.

Adsorption to the walls cannot be a dominating process in our experiments. If the chamber walls were highly adsorptive, they would act as a sink for vapors, and the aerosol would never achieve equilibrium. For example, in the experiments of Vaden et al.,[28] the SOA particles continuously evaporate because the chamber was filled with activated carbon to strip the vapors from the gas phase. If the walls in our chamber were efficient adsorbers, SOA particles would exhibit a similar behavior, but they do not. As shown in Figure 3, the condensation sink diameter is constant prior to the temperature perturbation, indicating that the aerosol is at equilibrium. When the temperature is increased, the particles initially evaporate and again approach a constant size indicating a new equilibrium state.

The second phenomenon could not occur in our experiments either. Since the aerosol was initially at equilibrium, the gas-phase could not be supersaturated with the vapors. Upon heating, the saturation ratios of the vapors in the gas phase drop even more.

Matsunaga and Ziemann[29] demonstrated that SVOCs can be lost to chamber walls by absorptive partitioning, which can occur at subsaturation conditions. In that case, the walls do not act as a sink for the vapors but exist at equilibrium with them. This phenomenon can have an important effect on the equilibrium gas-phase vapor concentrations and consequently on the net change in the condensation sink diameter. However, the time scale of gas-wall partitioning equilibration is on the order of a minute,[29] which is much shorter than the time scales of gas-particle partitioning measured in this study. Thus, gas-wall partitioning does not have a significant effect on the gas-particle partitioning equilibration time scales, which are the focus of this study.

3.3. Discussion and Comparison with Previous Studies. Our results show that when perturbed by a temperature step change, α-pinene SOA achieves gas-particle partitioning equilibrium. The equilibration time scales, at both low (~1 $\mu g/m^3$) and high (~100 $\mu g/m^3$) loadings, are consistent with a mass accommodation coefficient (α) on the

order of 0.1. In contrast to Vaden et al.[12] and Cappa and Wilson,[13] we did not observe evidence of extreme gas-particle partitioning inhibition due to diffusion limitations in the condensed phase. We note that neither of those studies measured equilibration time scales directly but inferred that equilibrium partitioning could not be achieved based on observed slow evaporation rates. However, evaporation rate measurements cannot constrain mass transfer limitations unless the volatility distribution is known, because both have an overlapping effect on evaporation rate. Vaden et al.[12] and Cappa and Wilson[13] used volatility distribution parametrizations derived from smog-chamber yield experiments[14] in their calculations. However, these volatility distributions likely do not represent the aged SOA due to formation of low volatility oligomers.[15,16] Consequently, it is possible that the reported condensed-phase diffusion limitations are misinterpretations of the low volatility of oligomers, as acknowledged by Cappa and Wilson.[13] Oligomer formation is associated with high glass transition temperatures, thus high viscosity[11] which potentially leads to slow condensed-phase diffusion. However, as stated above, we have not observed any substantial inhibition to gas-particle partitioning kinetics that can be attributed to slow diffusion.

To investigate the oligomer formation hypothesis, we compared our measured ΔC_{OA} values with those calculated using the volatility distribution parametrization of Pathak et al.[14] and enthalpy of vaporization parametrization of Epstein et al.[23] The calculated ΔC_{OA} values were on average a factor 5 and 3 larger than the measured values for high and low loading experiments, respectively. This suggests that the SOA is less volatile than fresh aerosol characterized by Pathak et al.;[14] therefore, low-volatility oligomers might indeed be responsible for the slow evaporation rates observed in previous studies.

Measuring the dynamic response of the aerosol in a closed system isolates the kinetics of gas-particle partitioning and mass transfer in the condensed-phase. The fact that equilibrium was achieved within the time scales of the experiments (minutes for high loadings and tens of minutes for low loadings) means that diffusion mass transfer time scales in the condensed-phase cannot be longer than the time scales of the experiments. We note that α accounts for both potential gas-phase and condensed-phase kinetic constraints, but we cannot distinguish between the two. Since $\alpha < 1$, it is possible that some resistance to mass transfer is caused by diffusion limitations in glassy or highly viscous SOA. However, the α found here (~0.1) is consistent with values reported for single-component dicarboxylic acids[19] where condensed-phase diffusion is not an issue. This suggests that the observed deviation from ideality ($\alpha = 1$) may not be due to condensed-phase mass transfer limitations.

3.4. Atmospheric Implications. Figure 5 plots equilibration time scales (τ) calculated using eq 3 and the accommodation coefficient (α) value we found for α-pinene SOA. We note that all α, D, and M combinations reported in Table 1 yield the same τ values. Calculations were performed for atmospherically relevant particle mass loadings (1−20 $\mu g/m^3$) and particle diameters ranging between 25 and 200 nm. As expected, for a constant particle mass loading, τ increases with increasing particle size because the condensation sink (CS) decreases. If the α values we report in this study for α-pinene SOA are representative of atmospheric SOA, then the equilibration time scales of atmospheric SOA range between minutes (for high loadings) and tens of minutes (for low loadings).

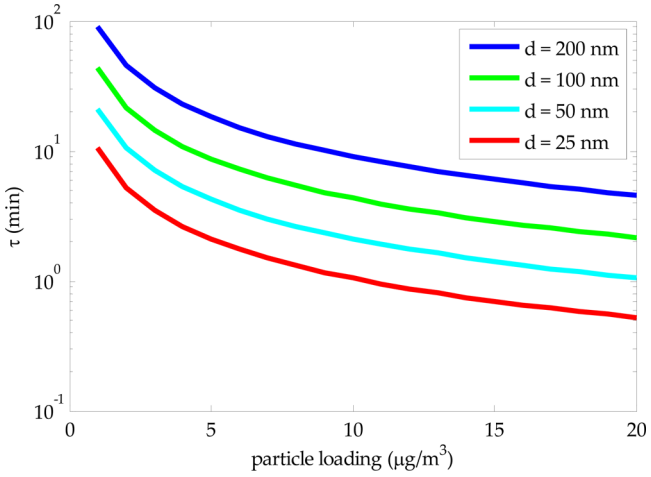

Figure 5. Equilibration time scales of atmospherically relevant particle loadings and sizes using α value found in this study (Table 1) for α-pinene SOA. Any combination of α, M, and D values in Table 1 gives the same results.

Under most circumstances equilibration time scales are less than 30 min, which supports the equilibrium assumption currently employed in most models. Certain rapid phenomena, such as plume dispersion, may require a more careful analysis of the condensation (or evaporation) dynamics, but these subgrid phenomena require special treatment in any event. One especially important phenomenon that often occurs at low loading (specifically low condensation sink) is new-particle formation and growth, but particles in nucleation experiments grow over many hours,[31] so even under these clean conditions the background (accumulation) mode can safely be assumed to be at equilibrium.

■ ASSOCIATED CONTENT

Supporting Information

The Supporting Information contains (1) description of the dependence of the mass accommodation coefficient on the gas phase diffusion coefficient and molar mass, (2) details of the treatment of wall-bound particles in the smog chamber perturbation experiments, and (3) derivation of the condensation sink diameter (d_{CS}). This information is available free of charge via the Internet at http://pubs.acs.org.

■ AUTHOR INFORMATION

Corresponding Author

*E-mail: alr@andrew.cmu.edu.

Notes

The authors declare no competing financial interest.

■ ACKNOWLEDGMENTS

Funding was provided by the U.S. Environmental Protection Agency National Center for Environmental Research (NCER) through the STAR program (R833748). The views, opinions, and/or findings contained in this article are those of the authors and should not be construed as an official position of the EPA.

■ REFERENCES

(1) Grieshop, A. P.; Miracolo, M. A.; Donahue, N. M.; Robinson, A. L. Constraining the volatility distribution and gas-particle partitioning of combustion aerosols using isothermal dilution and thermodenuder measurements. *Environ. Sci. Technol.* **2009**, *43*, 4750−4756.

(2) Valorso, R.; et al. Explicit modelling of SOA formation from α-pinene photooxidation: sensitivity to vapour pressure estimation. *Atmos. Chem. Phys.* **2011**, *11*, 6895−6910.
(3) Cappa, C. D.; Jimenez, J. L. Quantitative estimates of the volatility of ambient organic aerosol. *Atmos. Chem. Phys.* **2010**, *10*, 5409−5424.
(4) Huffman, J. a.; et al. Chemically-resolved aerosol volatility measurements from two megacity field studies. *Atmos. Chem. Phys. Discuss.* **2009**, *9*, 2645−2697.
(5) Donahue, N. M.; Robinson, a L.; Stanier, C. O.; Pandis, S. N. Coupled partitioning, dilution, and chemical aging of semivolatile organics. *Environ. Sci. Technol.* **2006**, *40*, 2635−43.
(6) Odum, J. R.; et al. Gas/Particle Partitioning and Secondary Organic Aerosol Yields. *Environ. Sci. Technol.* **1996**, *30*, 2580−2585.
(7) Saleh, R.; Shihadeh, A.; Khlystov, A. On transport phenomena and equilibration time scales in thermodenuders. *Atmos. Meas. Tech.* **2011**, *4*, 571−581.
(8) Wexler, A. S.; Seinfeld, J. H. The distribution of ammonium salts among a size and composition dispersed aerosol. *Atmos. Environ., Part A* **1990**, *24*, 1231−1246.
(9) Zobrist, B.; Marcolli, C.; Pedernera, D. A.; Koop, T. Do atmospheric aerosols form glasses? *Atmos. Chem. Phys. Discuss.* **2008**, 5221−5244.
(10) Virtanen, A.; et al. An amorphous solid state of biogenic secondary organic aerosol particles. *Nature* **2010**, *467*, 824−7.
(11) Koop, T.; Bookhold, J.; Shiraiwa, M.; Pöschl, U. Glass transition and phase state of organic compounds: dependency on molecular properties and implications for secondary organic aerosols in the atmosphere. *Phys. Chem. Chem. Phys.* **2011**, *13*, 19238−55.
(12) Vaden, T. D.; Imre, D.; Beránek, J.; Shrivastava, M.; Zelenyuk, A. Evaporation kinetics and phase of laboratory and ambient secondary organic aerosol. *Proc. Natl. Acad. Sci. U. S. A.* **2011**, *108*, 2190−5.
(13) Cappa, C. D.; Wilson, K. R. Evolution of organic aerosol mass spectra upon heating: implications for OA phase and partitioning behavior. *Atmos. Chem. Phys.* **2011**, *11*, 1895−1911.
(14) Pathak, R. K.; et al. Ozonolysis of α-pinene: parameterization of secondary organic aerosol mass fraction. *Atmos. Chem. Phys.* **2007**, *7*, 3811−3821.
(15) Hall, W. a.; Johnston, M. V. Oligomer Content of α-Pinene Secondary Organic Aerosol. *Aerosol Sci. Technol.* **2011**, *45*, 37−45.
(16) Tolocka, M. P.; et al. Formation of oligomers in secondary organic aerosol. *Environ. Sci. Technol.* **2004**, *38*, 1428−34.
(17) Saleh, R.; Khlystov, A.; Shihadeh, A. Determination of Evaporation Coefficients of Ambient and Laboratory-Generated Semivolatile Organic Aerosols from Phase Equilibration Kinetics in a Thermodenuder. *Aerosol Sci. Technol.* **2012**, *46*, 22−30.
(18) Perraud, V.; et al. Nonequilibrium atmospheric secondary organic aerosol formation and growth. *Proc. Natl. Acad. Sci. U. S. A.* **2012**, *109*, 2836−41.
(19) Saleh, R.; Shihadeh, A.; Khlystov, A. Determination of evaporation coefficients of semi-volatile organic aerosols using an integrated volume—tandem differential mobility analysis (IV-TDMA) method. *J. Aerosol Sci.* **2009**, *40*, 1019−1029.
(20) Davis, E. J. A history and state-of-the-art of accommodation coefficients. *Atmos. Res.* **2006**, *82*, 561−578.
(21) Li, W.; Davis, E. J. Aerosol Evaporation in the Transition Regime. *Aerosol Sci. Technol.* **1996**, *25*, 11−21.
(22) Hilal, S. H.; Karickhoff, S. W.; Carreira, L. a. Prediction of the Vapor Pressure Boiling Point, Heat of Vaporization and Diffusion Coefficient of Organic Compounds. *QSAR Comb. Sci.* **2003**, *22*, 565−574.
(23) Epstein, S. a; Riipinen, I.; Donahue, N. M. A semiempirical correlation between enthalpy of vaporization and saturation concentration for organic aerosol. *Environ. Sci. Technol.* **2010**, *44*, 743−8.
(24) Vehkamäki, H.; Riipinen, I. Thermodynamics and kinetics of atmospheric aerosol particle formation and growth. *Chem. Soc. Rev.* **2012**, *41*, 5160−73.
(25) Cappa, C. D. A model of aerosol evaporation kinetics in a thermodenuder. *Atmos. Meas. Tech.* **2010**, *3*, 579−592.
(26) Stanier, C. O.; Pathak, R. K.; Pandis, S. N. Measurements of the Volatility of Aerosols from α-Pinene Ozonolysis. *Environ. Sci. Technol.* **2007**, *41*, 2756−2763.
(27) Lehtinen, K. E. J.; Korhonen, H.; Maso, M. D. On the concept of condensation sink diameter. *Boreal Environ. Res.* **2003**, *8*, 405−411.
(28) Vaden, T. D.; Imre, D.; Beránek, J.; Shrivastava, M.; Zelenyuk, A. Evaporation kinetics and phase of laboratory and ambient secondary organic aerosol. *Proc. Natl. Acad. Sci. U. S. A.* **2010**, *108*, 1−6, DOI: 10.1073/pnas.1013391108.
(29) Matsunaga, A.; Ziemann, P. J. Gas-Wall Partitioning of Organic Compounds in a Teflon Film Chamber and Potential Effects on Reaction Product and Aerosol Yield Measurements. *Aerosol Sci. Technol.* **2010**, *44*, 881−892.
(30) Cocker, D. R., III; Clegg, S. L.; Flagan, R. C.; Seinfeld, J. H. The effect of water on gas−particle partitioning of secondary organic aerosol. Part I: α-pinene/ozone system. *Atmos. Environ.* **2001**, *35*, 6049−6072.
(31) Riipinen, I.; et al. The contribution of organics to atmospheric nanoparticle growth. *Nat. Geosci.* **2012**, *5*, 453−458.